# Atomic Process of Point Contact in Gold Studied by Time-Resolved High-Resolution Transmission Electron Microscopy

Tokushi Kizuka

*Department of Applied Physics, School of Engineering, Nagoya University, Furo-cho, Chikusa-ku, Nagoya, 464-8603, Japan*
*Research Center for Advanced Waste and Emission Management, Nagoya University, Furo-cho, Chikusa-ku, Nagoya, 464-8603, Japan*
*and PRESTO, JST, Nagoya University, Furo-cho, Chikusa-ku, Nagoya, 464-8603, Japan*

(Received 12 May 1998)

Contact and subsequent retraction between nanometer-sized gold tips were controlled at an atomic scale using a piezoelectric device at room temperature inside a high-resolution transmission electron microscope. The atomic process of the point contact was observed *in situ* at a spatial resolution of 0.2 nm and at a time resolution of $\frac{1}{60}$ s. It was shown that an atomistic pillarlike elongated neck is formed by lattice slip and structural relaxation during retraction. [S0031-9007(98)07641-8]

PACS numbers: 81.70.–q, 61.16.Bg, 62.20.Fe

Point contacts have been studied in terms of the following subjects: (1) initial processes of structural dynamics of mechanical interaction such as macroscopic contact, adhesion, friction, and fracture [1–4]; (2) the tip-sample interaction and resultant nanometer-sized structures in scanning probe microscopy (SPM) and related methods [5–12]; and (3) quantization and oscillation of conductance due to atomic scale constrictions [8,10–26]. Theoretical studies related to these subjects have been performed using the models defined by the area size and/or contact angle [14–17,22,26] and the models including atomic structures [1,3,11,19,24]. On the other hand, in experimental studies, point contacts were produced by the mechanically controllable break junction technique [18,23,25] and SPM [5–12]. However, the atomic process in structural dynamics of point contacts has not been shown experimentally, although it is fundamental to these studies. In the present study, contact and retraction were controlled at an atomic scale by piezodriving inside a high-resolution transmission electron microscope (HRTEM), and its atomic process was directly observed.

A piezodriving specimen holder of an HRTEM was developed for atomic scale mechanical contact and *in situ* observations [27]. Two needle-shaped specimens of polycrystalline gold were separately placed at the fixed and mobile sides of the specimen holder. The specimen holder was installed in a 200 kV HRTEM (JEOL, Ltd., JEM-2010). The two tips were contacted by controlling the piezodevice in the microscope at room temperature. Structural variation in the atomic arrangements was observed *in situ* using a silicon-integrated-target television camera and a digital video tape recorder. A time resolution of the system is $\frac{1}{60}$ s. The images shown in this study were averaged by two fields. The lattice resolution during the high-resolution observation using the present specimen holder was 0.14 nm. The electron irradiation density during the observation is $15 \times 10^4$ A/m$^2$. Actual increase in temperature of the specimen during the irradiation is less than 100 K [28].

Figures 1 and 2 show the time-sequence series of high-resolution images of the process of contact and retraction in the nanometer-sized gold tips, respectively. Each side of the specimen is connected to the mobile side [Fig. 1(a), *A*] and fixed side [Fig. 1(a), *B*] in the specimen holder. The tips are supported in a vacuum. The {111} and {200} lattice fringes of gold (lattice spacing, $d_{111} = 0.24$ nm and $d_{200} = 0.20$ nm) clearly appear during the contact in all areas of the tips *A* and *B*, respectively. The incident electron beam direction is parallel to the [110] axis of tip *A* and the [001] axis of tip *B*. The thickness of the contact area along the incident electron beam direction is inferred to be similar to the width along the perpendicular to the beam direction. It ranges at most up to a few nanometers. It is sufficiently thin for applying the weak phase object approximation to analyze the atomic arrangement of the area [29]. The atomic arrangement for Fig. 2(m) is shown schematically in Fig. 3.

First, the two tips are separated [Fig. 1(a)]. Tip *A* on the mobile side is displaced by the piezodriving to tip *B* on the fixed side. A few atomic columns emerge at the top of tip *A* [Fig. 1(b), small arrow] when the distance between the tips becomes less than 0.3 nm. Such emergence is never observed when the tips separate larger than the distance. Thus, the emergence shows that the tips are contacted with a boundary of a few atomic columns width. Atomic diffusion gives rise to the emergence, because the tips are not interacted mechanically at these positions. Such diffusion at nanometer-sized tips occurs due to the decrease in barrier height in addition to atomic force [5,30], and/or atomic emission in an electric field [31,32]. The latter is attributed to the electrostatic force which acts in the tips irradiated by electrons [33]. Tip *A* is then displaced in the same direction and the width of the contact boundary increases to about 1 nm [Fig. 1(c)]. The shape of the contact boundary differs from that of the overlapped image of

 0031-9007/98/81(20)/4448(4)$15.00 

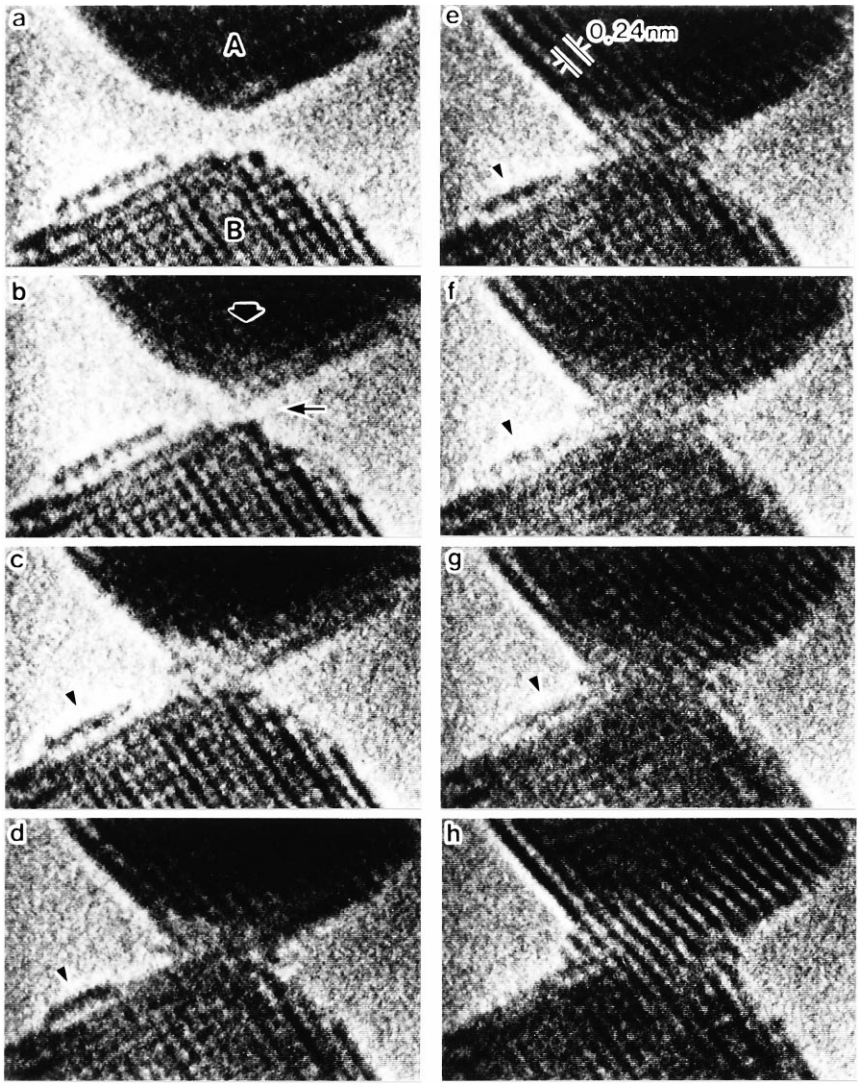


FIG. 1. Time-sequence series of high-resolution images of the formation of contact boundary and neck growth in the point contact of gold. Specimens are connected with the mobile (*A*) and fixed (*B*) sides of the piezodriving specimen holder. Time in each image is $\frac{0}{30}$ s (a), $\frac{90}{30}$ s (b), $\frac{93}{30}$ s (c), $\frac{110}{30}$ s (d), $\frac{116}{30}$ s (e), $\frac{117}{30}$ s (f), $\frac{118}{30}$ s (g), and $\frac{129}{30}$ s (h).

both tips. This shows that the structure of the contact boundary is stabilized at the contact. After the contact, the width of a terrace on tip *B* as shown by a triangle (▼) in Fig. 1(c) decreases, and the width of the contact boundary inversely increases [Figs. 1(c)–1(e)]. The atoms of the terrace migrate [Fig. 1(f)], and the terrace adheres to the contact boundary [Fig. 1(g)]. After the adhesion, all of the atoms of the terrace are absorbed into the contact boundary, resulting in the width of the contact boundary increasing to 2.5 nm [Fig. 1(h)]. This shows that the surface diffusion contributes to the neck growth in addition to compressive deformation. It was shown by Bitar *et al.* based on the Monte Carlo simulation that gold atoms move very fast along the nanometer cluster at room temperature; the barrier height for atom diffusion around the nanometer structures decreases [30]. The present observation in Figs. 1(f) and 1(g) directly shows such diffusion.

Lattice slip occurs on the {111} planes at the contact boundary when tip *A* is retracted by the piezodriving. The contact boundary elongates, while the width reduces every atomic layer during the slip [Figs. 2(i)–2(m)]. An atomistic pillarlike elongated neck is formed at the retraction. It is found from the present images that the atomic arrangement of the pillarlike neck is similar to that of the inner region of gold as shown in Fig. 3. The orientation of the pillarlike neck inclines by a few degrees relative to tip *A*. This is due to the relative shift of the tips along the direction perpendicular to the tensile direction. The formation of necks in macroscopic contacts in gold and copper wires was observed at room temperature at lower magnification by scanning electron microscopy and conventional transmission electron microscopy [4]. The neck elongation was also observed by SPM between the tip and the sample at room temperature without applying voltage to the tip [8] and at liquid helium temperature [10]. The electron irradiation and related increase of temperature hardly contribute to the formation of the pillarlike neck in the present study.

The width of the pillarlike neck decreases at the boundary between the neck and tip *B* as shown by the arrow in Fig. 2(n) after subsequent retraction [Figs. 2(n) and 2(o)]. Remarkable structural relaxation occurs around the pillarlike neck due to atomic diffusion just after the slip when the width decreases to less than about

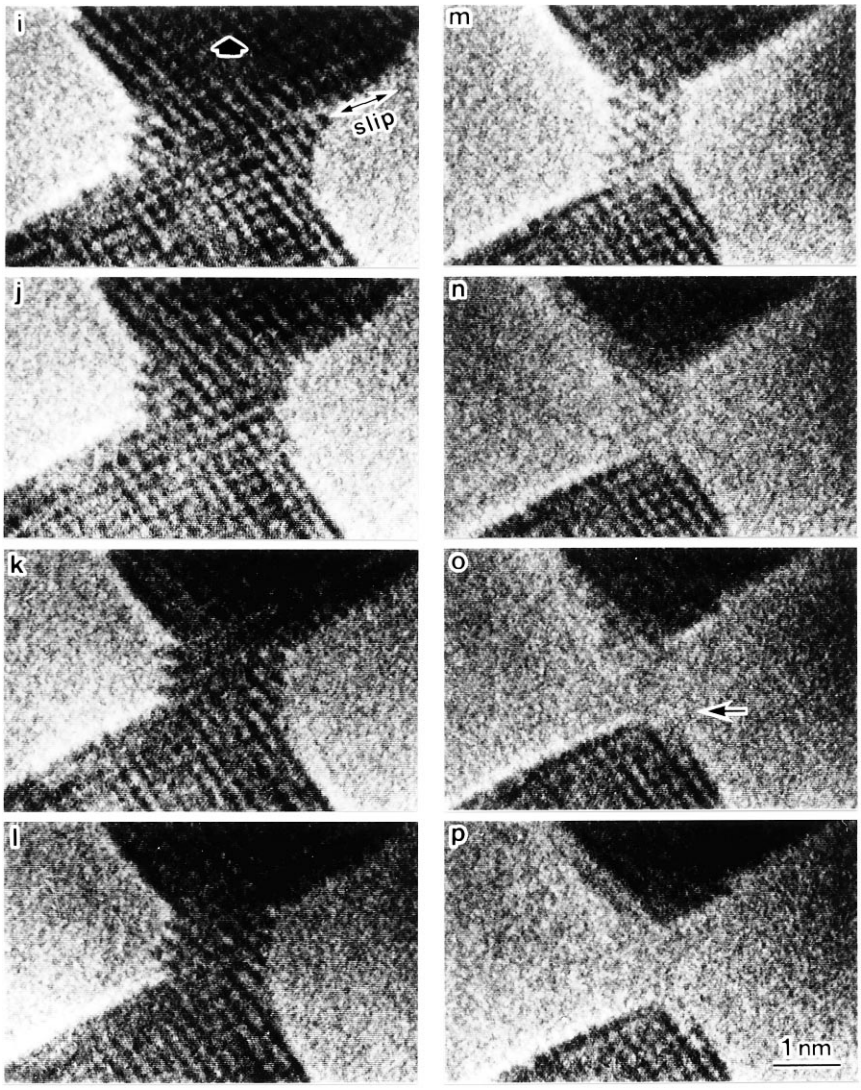


FIG. 2. Time-sequence series of high-resolution images of the formation and fracture of an atomistic pillarlike neck of gold during retraction. This process is the sequel to Fig. 1. The width of the pillarlike neck is shown by the number of the (002) atomic layers in upper tip (*A*); the number is 14 (i), 11 (j), 9 (k), 8 (l), and 5 (m). Time in each image is $\frac{210}{30}$ s (i), $\frac{230}{30}$ s (j), $\frac{240}{30}$ s (k), $\frac{250}{30}$ s (l), $\frac{270}{30}$ s (m), $\frac{280}{30}$ s (n), $\frac{290}{30}$ s (o), and $\frac{300}{30}$ s (p).

1 nm. Occasionally, the width recovers by the relaxation even when it decreases by one atomic column width by the slip. The period of the relaxation is $\frac{1}{60}$ s, or less. The pillarlike neck grows in the repeated process of the slip and subsequent relaxation. The molecular dynamics simulation in gold at 250 K also showed that the point contact area deformed in the repeated process of structural disorder transition and subsequent ordering [24]. Finally, the pillarlike neck breaks and disappears; the constituent atoms of the pillarlike neck migrate to both tips [Fig. 2(p)]. The shape of both tips as shown in Fig. 2(p) becomes sharp as compared with that before the contact as shown in Fig. 1(a). The tips elongate by 0.29 and 0.37 nm in tips *A* and *B*, respectively. The values correspond to lattice spacing of $(2\bar{2}0) \times 2$ and $(\bar{1}13) \times 3$, respectively. Such an elongation gives rise to the production of nanometer-sized dots by contact of the tip sample in SPM [8,10].

It is a problem whether the lattice slip proceeds by dislocation mechanism or simultaneous displacement of lattices at the point contacts, although the definition of dislocation is difficult at such small regions. In the present study, the introduction of a dislocation or dislocationlike localized strain could not be confirmed in the pillarlike neck less than 2 nm width between the tips of different orientation. Agraït *et al.* reported that the value of the yield strength in the deformation of the point contact between gold tips was up to 20 times larger than the macroscopic value, when the diameter of the contact area was reduced from 16 to 8 nm [10], suggesting that the dislocation was absent before the deformation and/or was not introduced during the deformation [34,36]. On the other hand, it was reported that, in a single crystalline gold of about 4 nm width, partial dislocations were introduced during the deformation at room temperature [37]. In the molecular dynamics simulation of deformation in rhodium at room temperature, a dislocation was introduced and moved during the deformation [3]. In addition to the present atomistic observation, the yield strength of the slip should be measured directly in order to elucidate the slip mechanism.

In the present method, such an approach-contact-deformation-fracture process at point contact can be observed repeatedly. No dislocation is observed in the

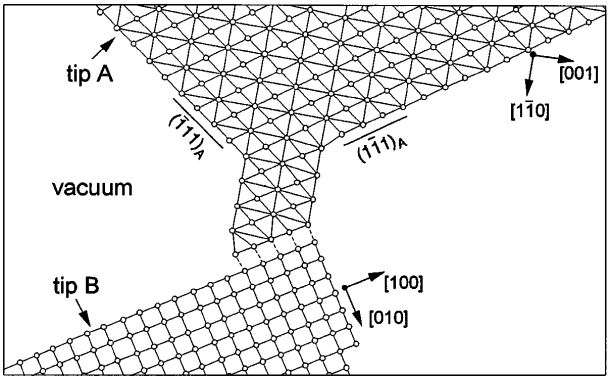


FIG. 3. Illustration of projected atomic arrangement for Fig. 2(m). Tips *A* and *B* connect with the mobile side and fixed side of the piezodriving specimen holder, respectively. Solid lines and dotted lines show atomic bonds in the tips and at a orientational boundary, respectively.

pillarlike necks after the formation though it is not clear whether dislocations are introduced or not during the slip. This shows that fatigue due to pileup of dislocations never occurs in atomic pillarlike necks [34–36]. It is deduced that the pillarlike necks have high strength and toughness when they are used as nanometer-sized materials such as single electron devices.

In conclusion, the atomic process of the point contact in gold is directly observed by HRTEM using the piezodriving specimen holder. The elemental processes are (1) the formation of the contact boundary of a few atomic columns width at the first contact, (2) the neck growth due to the compressive deformation and surface diffusion, (3) the formation of the atomistic pillarlike necks by the slip deformation and structural relaxation during the retraction, and (4) the fracture and disappearance of the pillarlike necks. The top of the tips elongates by a few atomic layers after the process.

The author thanks Mikio Naruse and Shunji Deguchi of JEOL Ltd. for help with the production of the piezodriving HRTEM specimen holder. The author also acknowledges Dr. Satoru Fujisawa of the Mechanical Engineering Laboratory of Ministry of International Trade and Industry for providing useful information about point contact. Financial support was provided for the present study from the TEPCO Research Foundation, Kawasaki Steel 21st Century Foundation, and the Sumitomo Foundation. The present study was partly supported by a Grant-In-Aid from the Ministry of Education, Science, Sports and Culture.

[1] U. Landman, W. D. Luedtke, N. A. Burnham, and R. J. Colton, Science **248**, 454 (1990).
[2] A. Stalder and U. Dürig, J. Vac. Sci. Technol. B **14**, 1259 (1996).
[3] R. M. Lynden-Bell, Science **263**, 1704 (1994).
[4] A. Correia and N. García, Phys. Rev. B **55**, 6689 (1997).
[5] G. Binnig, C. F. Quate, and Ch. Gerber, Phys. Rev. Lett. **56**, 930 (1986).
[6] C. M. Mate *et al.*, Phys. Rev. Lett. **59**, 1942 (1987).
[7] J. K. Gimzewski and R. Möller, Phys. Rev. B **36**, 1284 (1987).
[8] J. I. Pascual *et al.*, Phys. Rev. Lett. **71**, 1852 (1993).
[9] L. Kuipers and J. W. Frenken, Phys. Rev. Lett. **70**, 3907 (1993).
[10] N. Agraït, G. Rubio, and S. Vieira, Phys. Rev. Lett. **74**, 3995 (1995).
[11] J. I. Pascual *et al.*, Science **267**, 1793 (1995).
[12] J. L. Costa-Krämer *et al.*, Phys. Rev. B **55**, 5416 (1997).
[13] B. J. van Wees *et al.*, Phys. Rev. Lett. **60**, 848 (1988).
[14] N. García and L. Escapa, Appl. Phys. Lett. **54**, 1418 (1989).
[15] E. G. Haanappel and D. van der Marel, Phys. Rev. B **39**, 5484 (1989).
[16] M. Yosefin and M. Kaveh, Phys. Rev. Lett. **64**, 2819 (1990).
[17] E. Tekman and S. Ciraci, Phys. Rev. B **43**, 7145 (1991).
[18] C. J. Muller, J. M. van Ruitenbeek, and L. J. de Jongh, Phys. Rev. Lett. **69**, 140 (1992).
[19] T. N. Todorov and A. P. Sutton, Phys. Rev. Lett. **70**, 2138 (1993).
[20] L. Olesen *et al.*, Phys. Rev. Lett. **72**, 2251 (1994).
[21] N. Agraït, J. G. Rodrigo, and S. Vieira, Phys. Rev. B **47**, 12 345 (1993).
[22] J. A. Torres, J. I. Pascual, and J. J. Sáenz, Phys. Rev. B **49**, 16 581 (1994).
[23] J. M. Krans *et al.*, Nature (London) **375**, 767 (1995).
[24] A. M. Bratkovsky, A. P. Sutton, and T. N. Todorov, Phys. Rev. B **52**, 5036 (1995).
[25] C. Zhou *et al.*, Appl. Phys. Lett. **67**, 1160 (1995).
[26] J. A. Torres and J. J. Sáenz, Phys. Rev. Lett. **77**, 2245 (1996).
[27] T. Kizuka *et al.*, Phys. Rev. B **55**, R7398 (1997).
[28] S. Iijima, *Microclusters*, edited by S. Sugano, Y. Nishina, and S. Onishi (Springer-Verlag, Berlin, 1986), p. 186.
[29] S. Horiuchi, in *Fundamentals of High-Resolution Transmission Electron Microscopy* (North-Holland, Amsterdam, 1994), Chap. 6, p. 149.
[30] L. Bitar *et al.*, Surf. Sci. **339**, 221 (1995).
[31] V. T. Binh and N. García, Ultramicroscopy **42–44**, 80 (1992).
[32] C. X. Guo and D. J. Thomson, Ultramicroscopy **42–44**, 1452 (1992).
[33] T. Kizuka *et al.*, J. Electron Microsc. **2**, 151 (1997).
[34] A. H. Cottrell, in *Theory of Crystal Dislocations* (Gordon and Breach, New York, 1964).
[35] J. P. Hirth and J. Lothe, in *Theory of Dislocations* (McGraw-Hill, New York, 1968).
[36] F. R. N. Nabarro, in *Crystal Dislocations* (Oxford Clarendon, New York, 1968).
[37] T. Kizuka, Phys. Rev. B **57**, 11 158 (1998).